Zdzisław Pisarek
Rzeszow University of Technology
Faculty of Civil and Environmental Engineering

EXPERIMENTAL TESTS OF T- STUBS WITH FOUR BOLTS

In the most common framed structures end-plate connections are utilized. In this joints are apply only two bolt rows in the tension zone with two bolts in each row. When the beam is made from H section, designers apply joints with four bolts in each row. Design rules given in Eurocode 3 relate only to bolted end-plate joints with two bolts in each bolt row. The present paper is concerned with experimental tests of welded T-stubs with four bolts. A comparison of test results with an analytical model for T-stub with four bolts is presented.

Key words: end-plate connection, T-stub, experimental investigation, component method, mechanical model.

У поширених стержневих системах використовуються торцеві з'єднання. В цих з'єднаннях застосовується два ряди болтів у розтягнутій зоні з двома болтами в кожному ряді. Коли балка виготовлена з Н-профілю, проектанти застосовують з'єднання з чотирма болтами в ряді. Норми проектування Єврокод 3 нормують лише болтове торцеве з'єднання з двома болтами в кожному ряді болтів. Дана стаття присвячена випробуванням звареного Т-коротиша з чотирма болтами. Порівняно результати випробувань з аналітичною моделлю.

Ключові слова: торцеве з'єднання, Т-коротиш, експериментальні дослідження, компонентний метод, механічна модель.

Introduction

Bolted end-plate moment connections are often used in unbraced steel frame structures. These types of joints are mainly applied to connect beams to columns and as beam splices. Increase of the resistance of the joints can be achieved by applying additional bolts row, however additional bolts row have a rather small participation in the resistance of the whole joint. When great moment resistance of the joint is required, designers apply connections with four bolts in each row. The design rules given in Eurocode 3 [1] relate to bolted end plate joint with only two bolts in each row.

The analytical models for analysis of multiple row end-plate joints with four bolts in the row are based on three main methods [2]: yield line theory, bolt force determination and component method preferred in Eurocode 3. In this method, resistance of tension zone of the joint is modeled by equivalent T-stub. The deformations and strength of the equivalent T-stubs with four bolts can be predicted according to the different methods [2],[3],[4]. The difference between these methods is seen mainly in the statical scheme of part of the end-plate plate.

Verification of the analytical method and to find failure modes should be carrying by experimental tests.

Analytical model for T-stub with four bolts

Based on the behaviour of the preliminary test specimen a simple beam model was development. The resistance and deformations of the T-stub depends on the strength of the bolts, thickness of the end-plate and geometrical dimensions of the T-stub. The possible modes of failure are presented in fig. 1 [2].

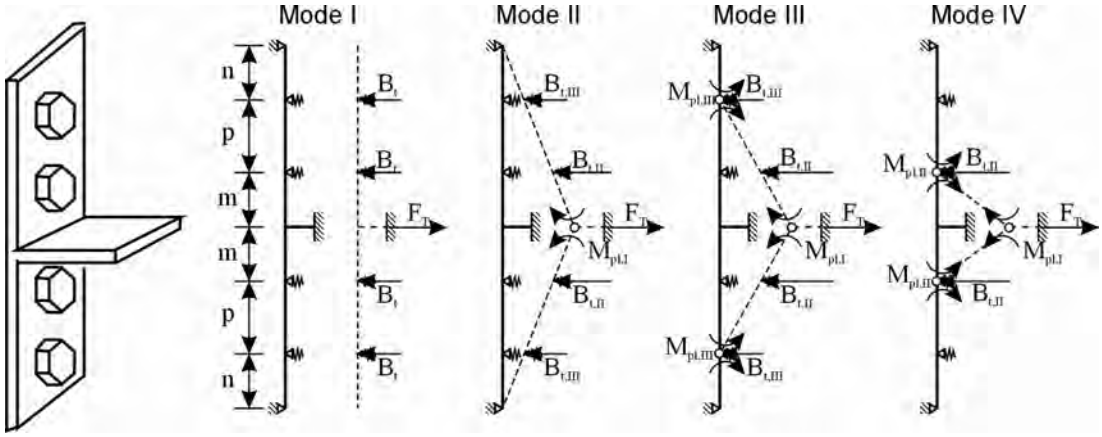

Fig. 1. Analytical model for T-stub with four bolts

The equations for calculations of the resistance and stiffness coefficients of the T-stub are collected in table 1.

Table 1

Resistance and stiffness coefficient of T-stubs with four bolts

mode of failure	resistance	Stiffness coefficient
I	$F_{T,1,Rd} = \quad B_{t.Rd}$	$k_{T,1} = 3,2 \cdot \frac{A_s}{L_b^p}$
II	$F_{T,2,Rd} = \frac{2 \cdot M_{pl,I,Rd} + (4 \cdot n + 2 \cdot p) \cdot B_{t.Rd}}{m + p + n}$	$k_{T,2} = \frac{1}{\frac{(n+p) \cdot L_b^p}{1,6 \cdot (2 \cdot n + p) \cdot A_s} + \frac{m^3}{0,9 \cdot l_{eff} \cdot t_p^3}}$
III	$F_{T,3,Rd} = \frac{2 \cdot M_{pl,I,Rd} + 2 \cdot M_{pl,III,Rd} + 2 \cdot p \cdot B_{t.Rd}}{m + p}$	$k_{T,2} = \frac{1}{\frac{L_b^p}{1,6 \cdot A_s} + \frac{m^3}{0,9 \cdot l_{eff} \cdot t_p^3}}$
IV	$F_{T,4,Rd} = \frac{2 \cdot M_{pl,I,Rd} + 2 \cdot M_{pl,II,Rd}}{m}$	$k_{T,4} = \frac{0,9 \cdot l_{eff} \cdot t_p^3}{m^3}$

Experimental tests

On the basis of analytical model the parametric analysis of the influence of individual components on the resistance and deformations of the T-stub was performed. Fixed also independent parameters influence on characteristics of the connection. As variable parameters the geometric measurements of T-stub and the strength of bolts was accepted. For reduce number of variable parameters assumed that the bolt diameter is constant and their strength will be changed depending only on their class.

Experimental tests were carried out on welded T-stub specimen. To the preparation of specimens one the experiment plan according to Hartley PS/DS-P:Ha_6 based on the hypercube [5] was adopted. As variable parameters was chosen 6 parameters with ranges of their variability (Table 2):

– bolt end distance e = (16 – 40) mm
– bolt spacing p = (35 – 65) mm
– inner bolts and web distance m = (16 – 44) mm
– T-stub flange width b_p = (50-150) mm
– thickness of the T-stub flange t_p = (10 -30) mm
– bolts grade g_b = (5.8-10.9)

The tests conducted on Instron Bluehill 1200kN ISRS testing machine. The load was applied with constant speed of 3 mm/min. During tests tensile force and total deformation of the T-stub were measured. The form of the deformation of the specimen under load was also observed. The example T-stub on the testing machine is presented in fig. 2.

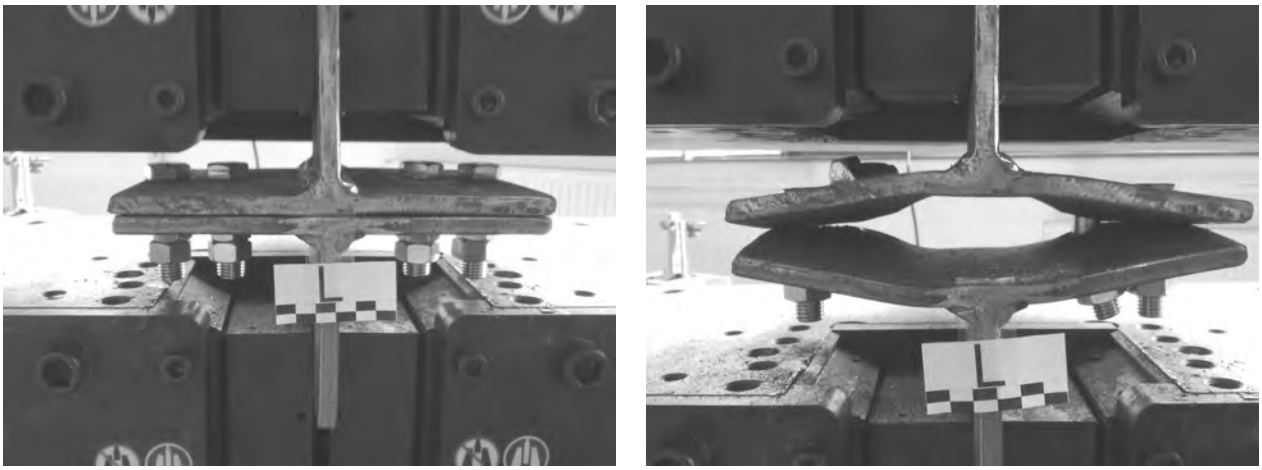

Fig. 2. T-stub specimen on testing machine before test and in final test moment

Table 2

Variable parameters of specimens according to Hartley PS/DS-P:Ha6 experiment plan

No.	specimen	$\hat{x}_1$	$\hat{x}_2$	$\hat{x}_3$	$\hat{x}_4$	$\hat{x}_5$	$\hat{x}_6$	e	p	m	b_p	t_p	g_b
1	A	+1	+1	+1	+1	+1	+1	40	65	44	150	30	10.9
2	B	+1	+1	+1	-1	+1	-1	40	65	44	50	30	5.8
3	C	+1	+1	+1	-1	-1	+1	40	65	44	50	10	10.9
4	D	+1	+1	+1	+1	-1	-1	40	65	44	150	10	5.8
5	E	-1	+1	-1	+1	+1	+1	16	65	16	150	30	10.9
6	F	-1	+1	-1	-1	+1	-1	16	65	16	50	30	5.8
7	G	-1	+1	-1	-1	-1	+1	16	65	16	50	10	10.9
8	H	-1	+1	-1	+1	-1	-1	16	65	16	150	10	5.8
9	I	-1	-1	+1	+1	+1	+1	16	35	44	150	30	10.9
10	J	-1	-1	+1	-1	+1	-1	16	35	44	50	30	5.8
11	K	-1	-1	+1	-1	-1	+1	16	35	44	50	10	10.9
12	L	-1	-1	+1	+1	-1	-1	16	35	44	150	10	5.8
13	Ł	+1	-1	-1	+1	+1	+1	40	35	16	150	30	10.9
14	M	+1	-1	-1	-1	+1	-1	40	35	16	50	30	5.8
15	N	+1	-1	-1	-1	-1	+1	40	35	16	50	10	10.9
16	O	+1	-1	-1	+1	-1	-1	40	35	16	150	10	5.8
17	P	$+\alpha$	0	0	0	0	0	40	50	30	100	20	8.8
18	Q	$-\alpha$	0	0	0	0	0	16	50	30	100	20	8.8
19	R	0	$+\alpha$	0	0	0	0	28	65	30	100	20	8.8
20	S	0	$-\alpha$	0	0	0	0	28	35	30	100	20	8.8
21	T	0	0	$+\alpha$	0	0	0	28	50	44	100	20	8.8
22	U	0	0	$-\alpha$	0	0	0	28	50	16	100	20	8.8
23	V	0	0	0	$+\alpha$	0	0	28	50	30	150	20	8.8
24	W	0	0	0	$-\alpha$	0	0	28	50	30	50	20	8.8
25	X	0	0	0	0	$+\alpha$	0	28	50	30	100	30	8.8
26	Y	0	0	0	0	$-\alpha$	0	28	50	30	100	10	8.8
27	Z	0	0	0	0	0	$+\alpha$	28	50	30	100	20	10.9
28	Ż	0	0	0	0	0	$-\alpha$	28	50	30	100	20	5.8
29	Ź	0	0	0	0	0	0	28	50	30	100	20	8.8

Results of the experimental tests

During the tests all defined modes of failure were observed. The difference between modes of failure can be observed on the tensile force – deformation characteristics. The characteristics for different modes are presented in fig 3 to 31. In table 3 the results of the experimental tests are presented.

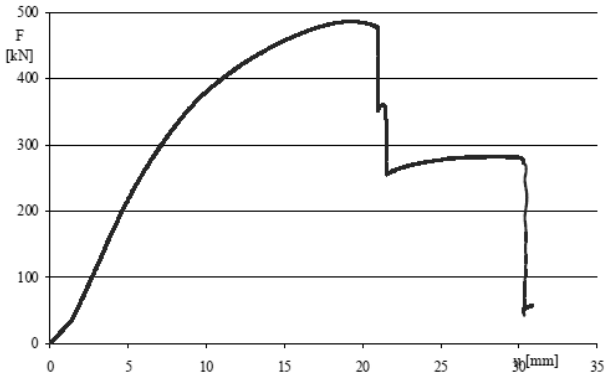

Fig. 3. Specimen A – II mode of failure

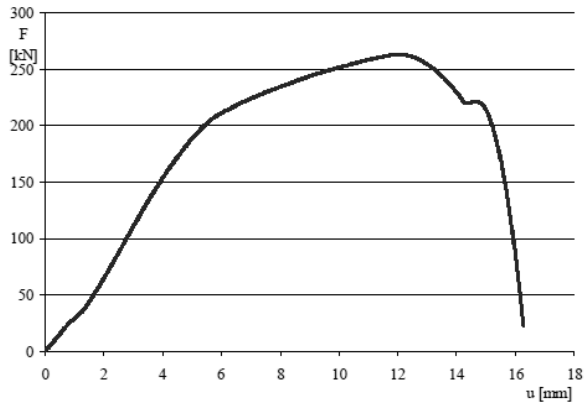

Fig. 4. Specimen B – I mode of failure

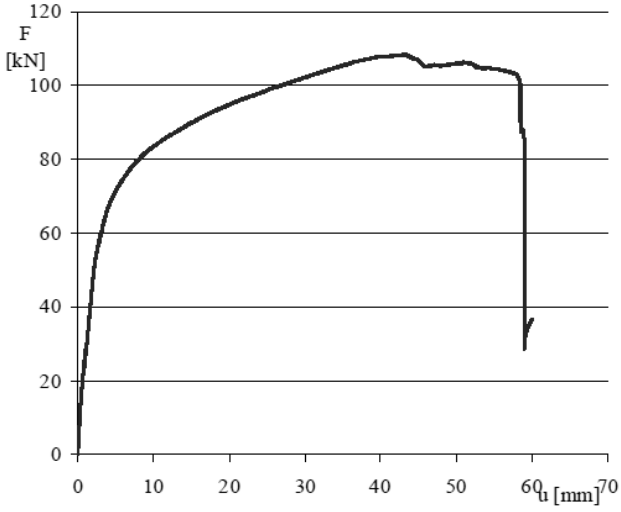

Fig. 5. Specimen C – IV mode of failure

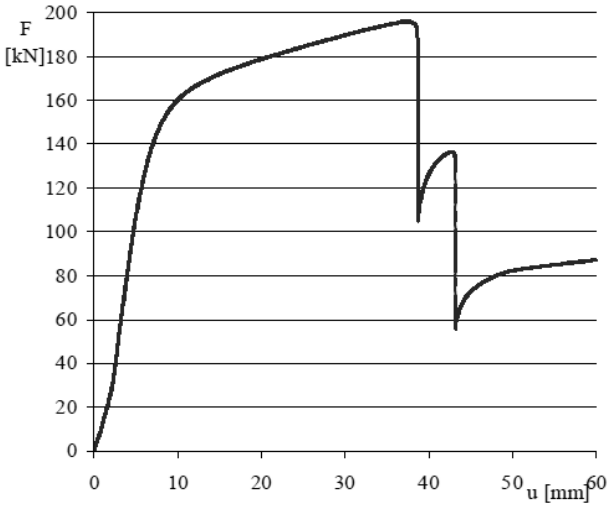

Fig. 6. Specimen D – III mode of failure

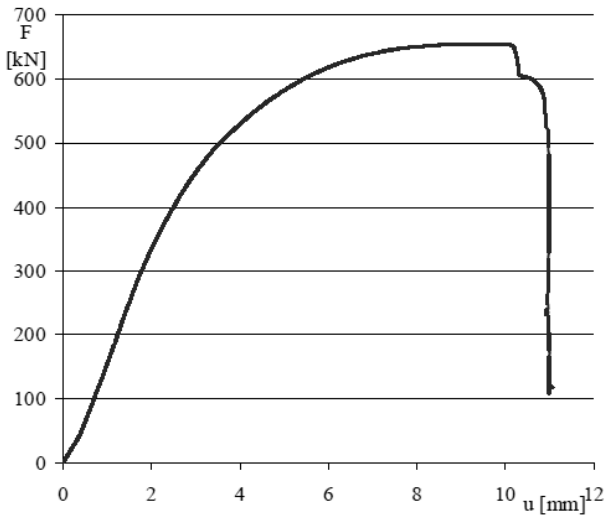

Fig. 7. Specimen E – I mode of failure

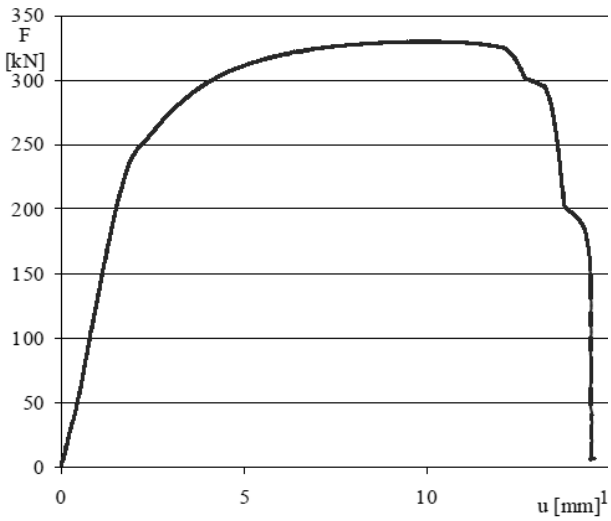

Fig. 8. Specimen F – I mode of failure

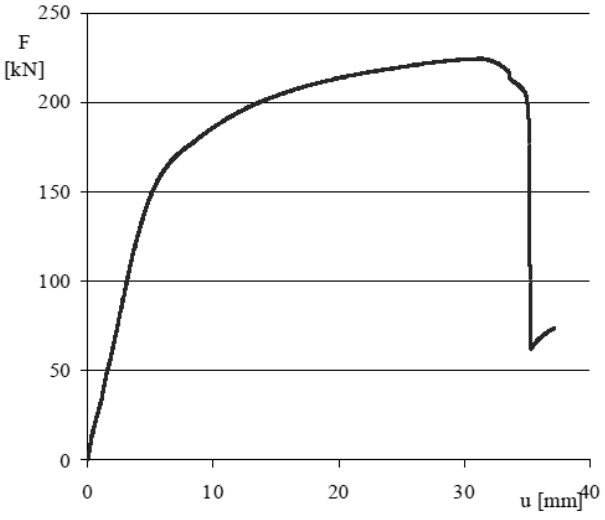

Fig. 9. Specimen G – IV mode of failure

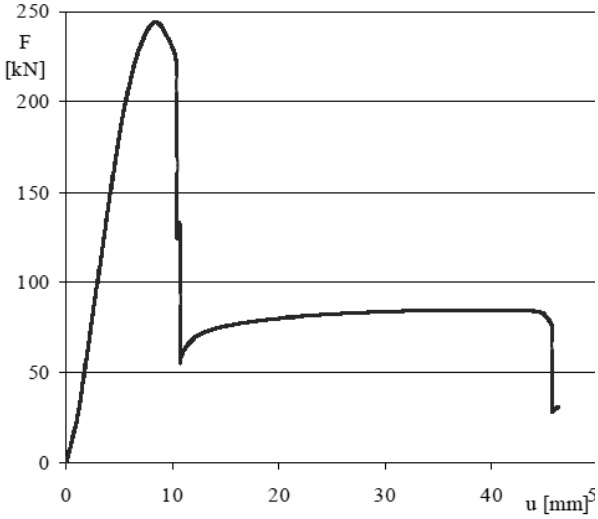

Fig. 10. Specimen H – III mode of failure

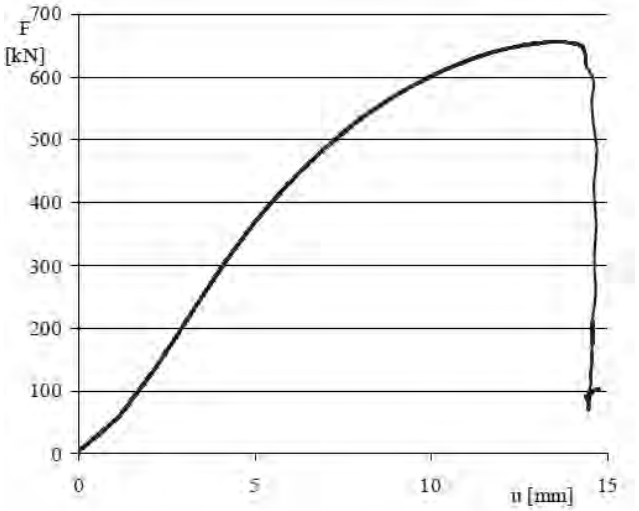

Fig. 11. Specimen I – I mode of failure

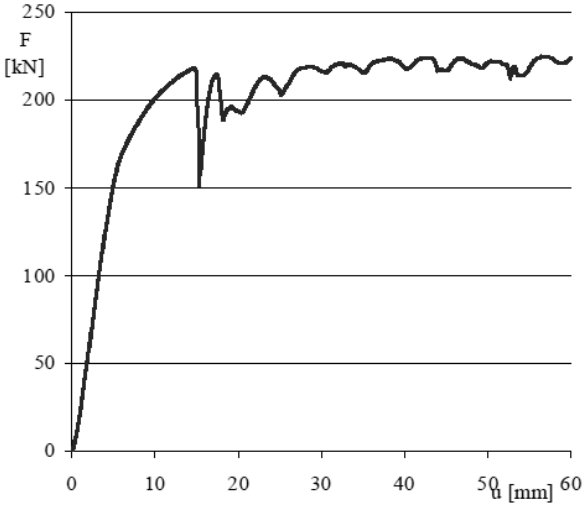

Fig. 12. Specimen J – I mode of failure

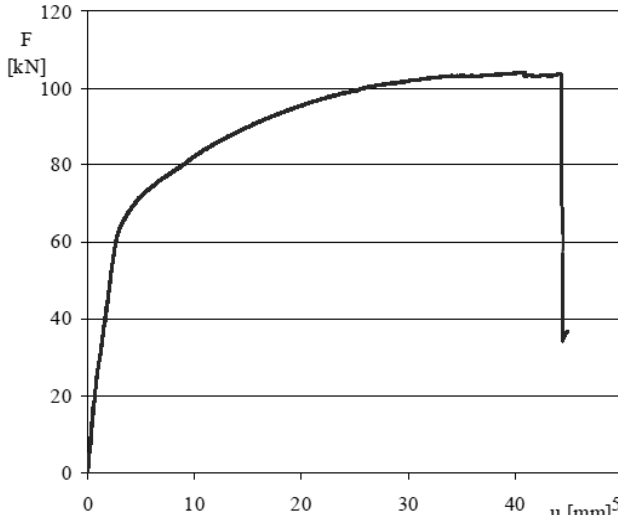

Fig. 13. Specimen K – IV mode of failure

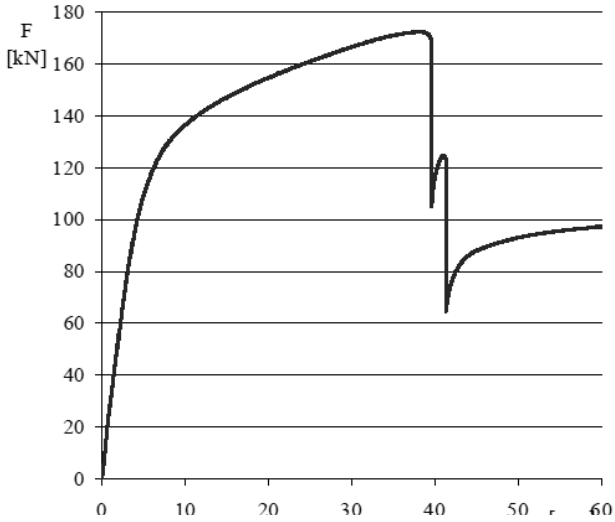

Fig. 14. Specimen L – III mode of failure

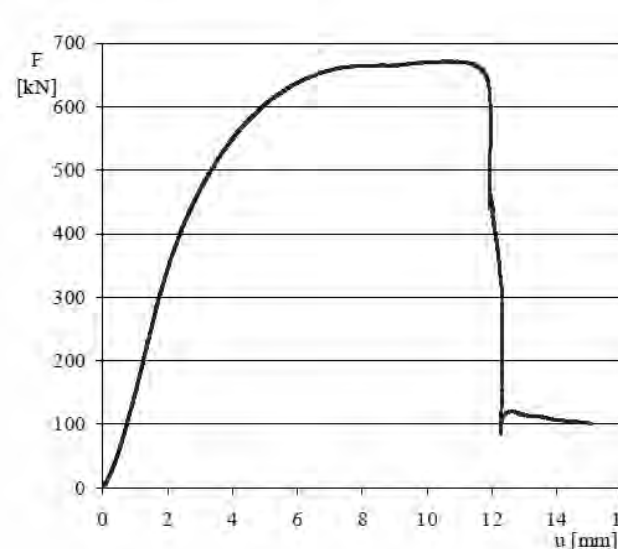

Fig. 15. Specimen Ł – I mode of failure

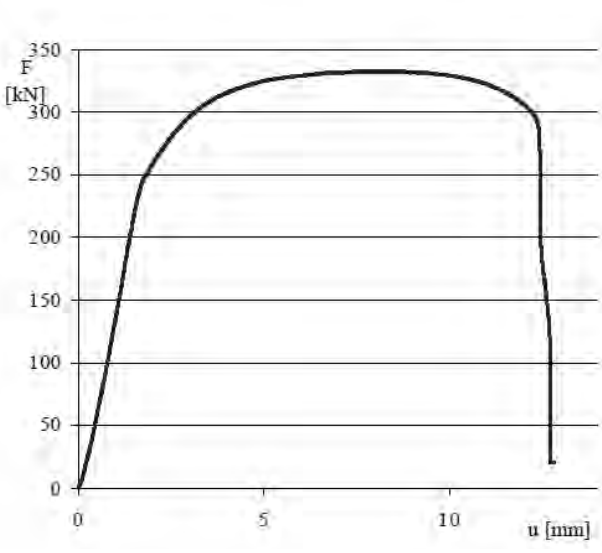

Fig. 16. Specimen M – I mode of failure

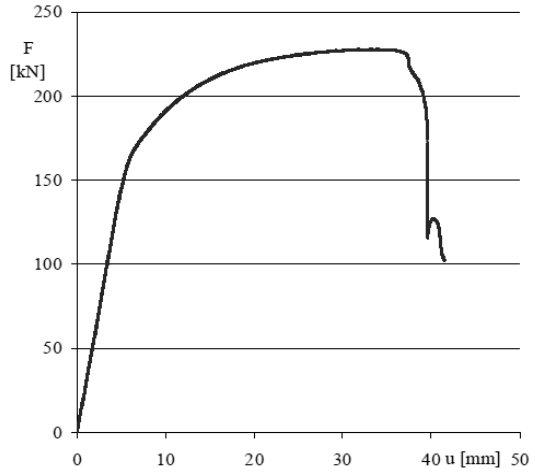

Fig. 17. Specimen N – IV mode of failure

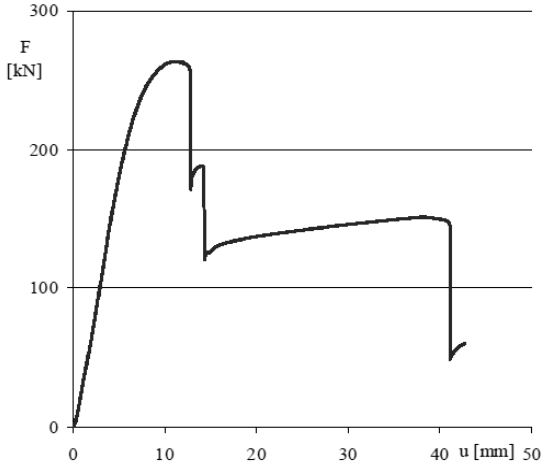

Fig. 18. Specimen O – III mode of failure

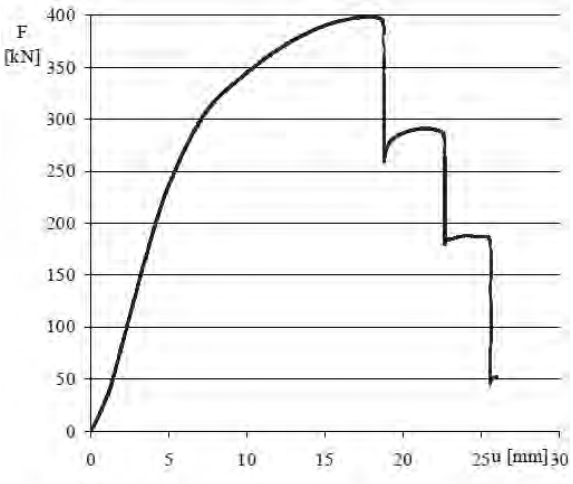

Fig. 19. Specimen P – II mode of failure

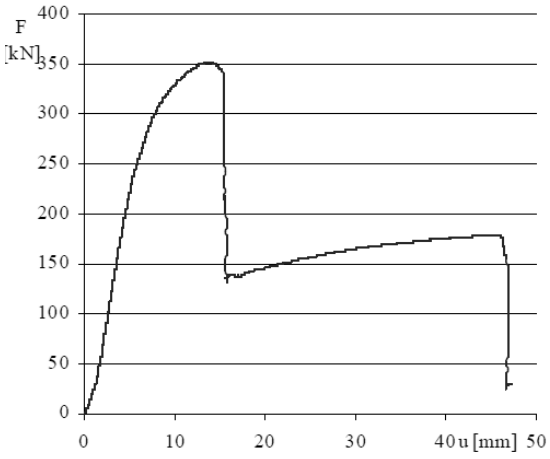

Fig. 20. Specimen Q – II mode of failure

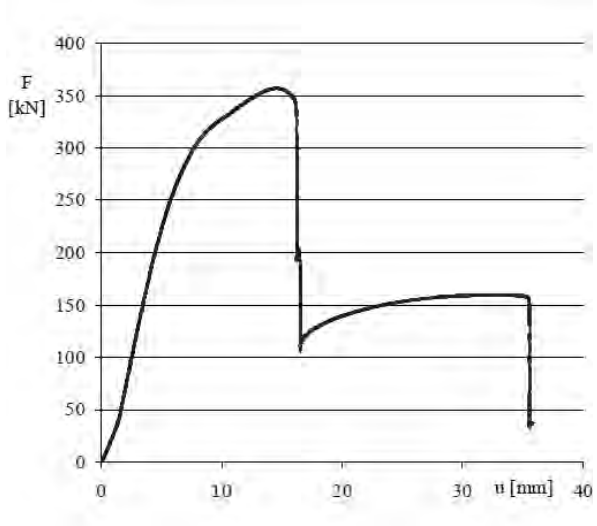

Fig. 21. Specimen R – II mode of failure

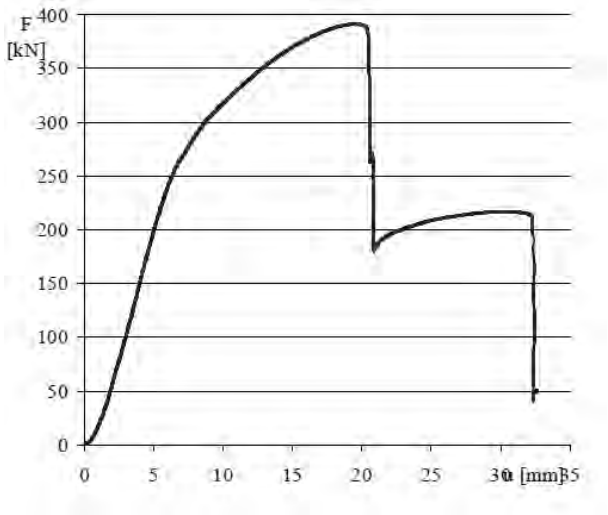

Fig. 22. Specimen S – II mode of failure

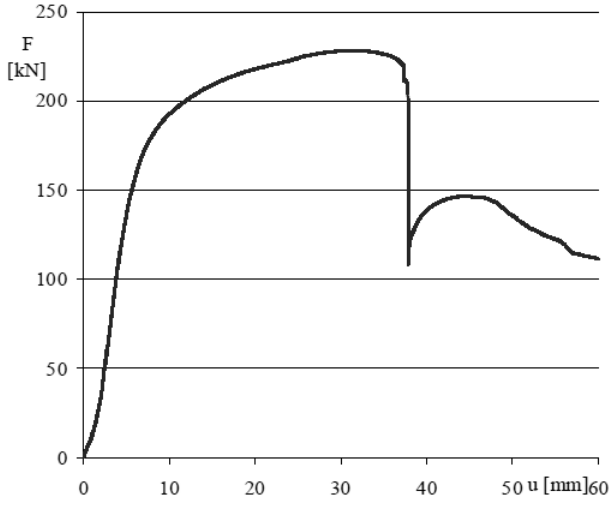

Fig. 23. Specimen T – IV mode of failure

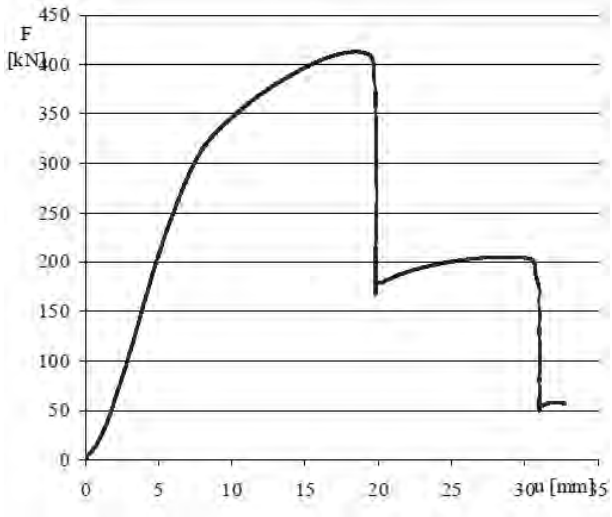

Fig. 24. Specimen U – II mode of failure

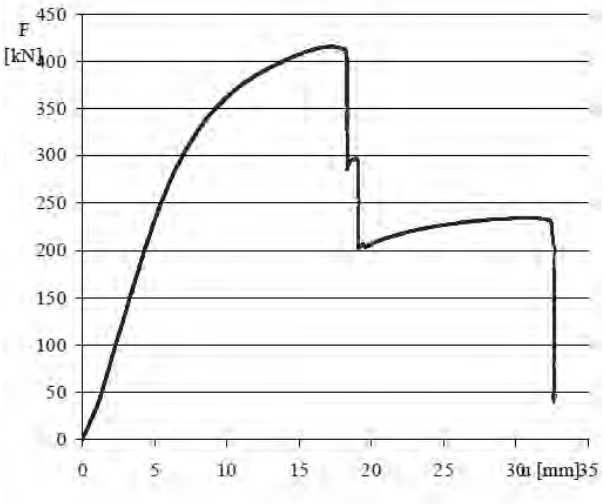

Fig. 25. Specimen V – II mode of failure

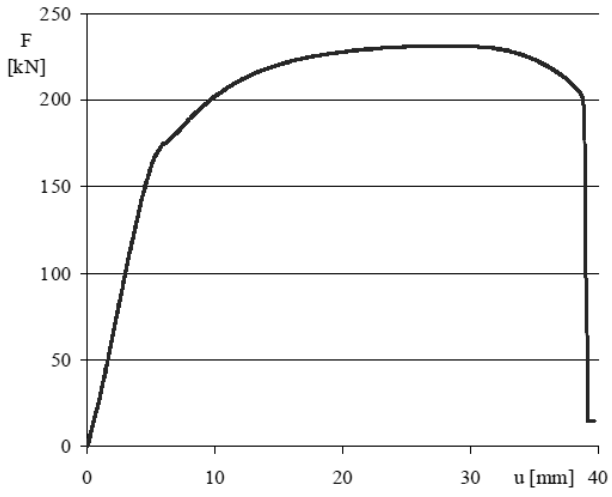

Fig. 26. Specimen W – III mode of failure

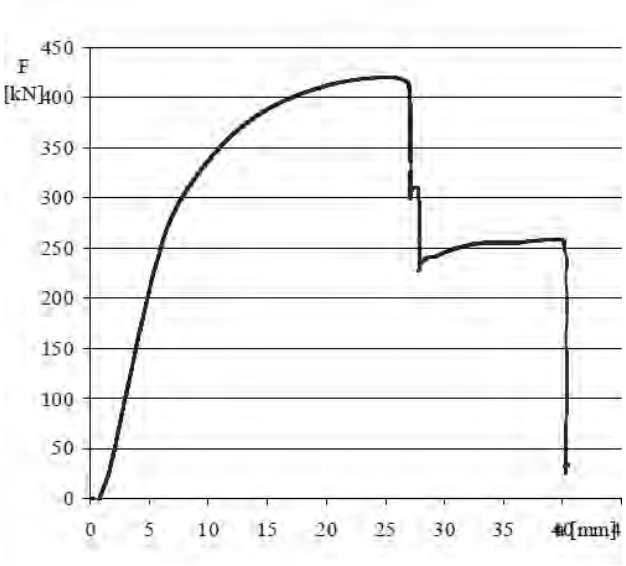

Fig. 27. Specimen X – II mode of failure

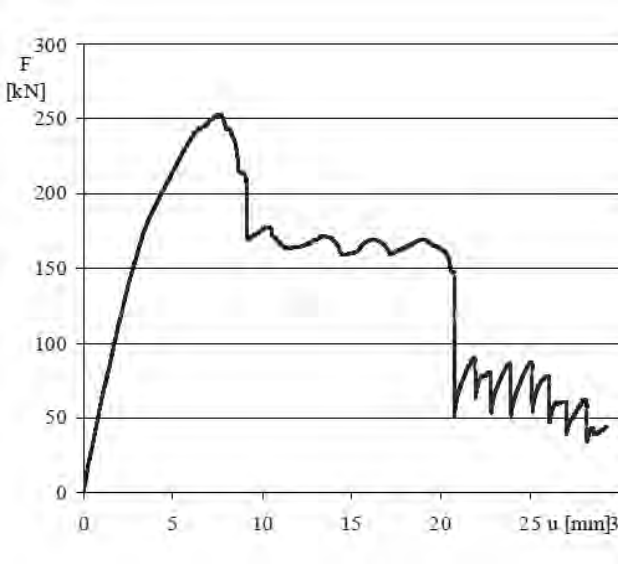

Fig. 28. Specimen Y – IV mode of failure

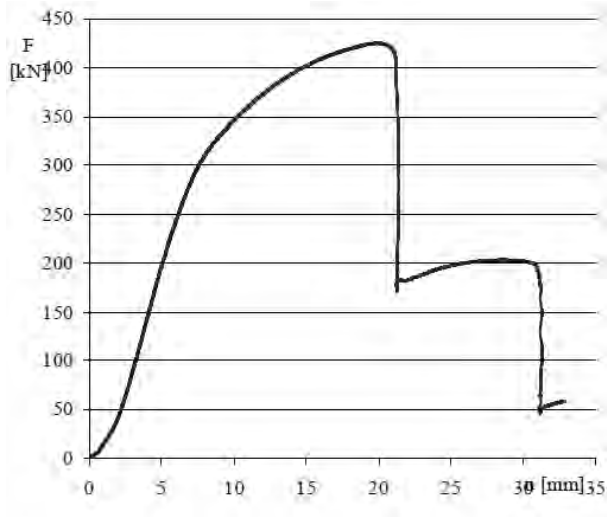

Fig. 29. Specimen Z – II mode of failure

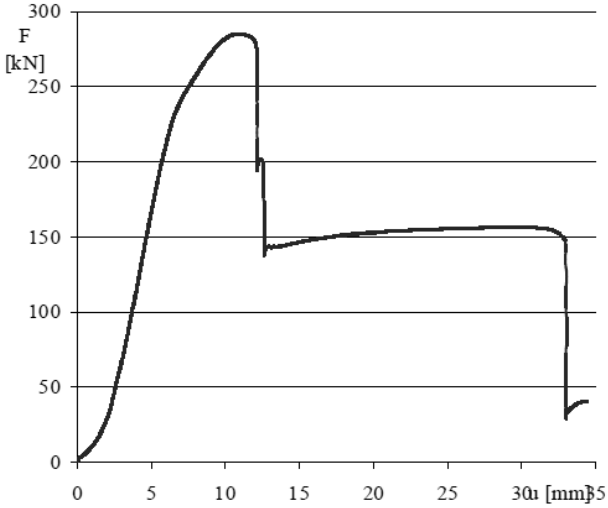

Fig. 30. Specimen Ż – II mode of failure

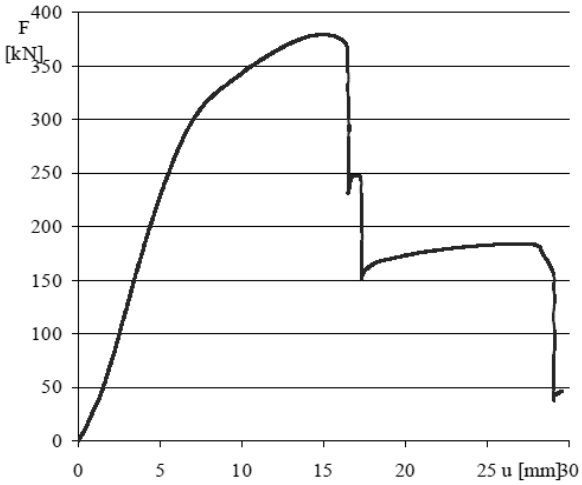

Fig. 31. Specimen Ź – II mode of failure

Table 3

Mean values of dimension and maximum tensile force from test machine of the specimens.

No	Speci-men	Mean values of real dimensions					test		analytical model	
		e	p	m	b_p	t_p	force [kN]	mode of failure	force [kN]	mode of failure
1	A	40,09	65,01	44,36	150,00	30,37	486,7	II	455,1	II
2	B	40,09	65,38	44,21	50,83	30,35	263,5	I	205,4	II
3	C	41,61	64,60	44,03	49,68	10,03	108,4	IV	33,8	IV
4	D	41,03	64,50	44,26	149,02	10,08	195,9	III	101,9	IV
5	E	15,19	65,01	16,19	151,38	30,15	654,8	I	535,9	II
6	F	15,44	65,15	16,64	52,53	30,28	330,1	I	235,1	II
7	G	16,93	65,00	16,51	49,34	10,01	224,5	IV	89,2	IV
8	H	16,83	64,38	16,33	149,05	10,07	244,3	III	186,0	III
9	I	16,36	35,14	44,33	151,28	30,48	656,4	I	449,7	II
10	J	16,28	35,25	44,28	51,69	30,33	224,8	I	189,5	II
11	K	16,50	34,76	43,89	50,17	10,48	104,2	IV	37,4	IV
12	L	16,75	35,28	43,72	150,35	10,13	172,5	III	105,2	IV
13	Ł	39,66	35,65	11,43	151,71	30,38	672,2	I	653,1	I
14	M	39,53	35,33	16,02	52,20	30,40	332,6	I	284,6	II
15	N	41,53	36,08	15,93	49,35	10,07	227,8	IV	93,6	IV
16	O	40,14	35,81	15,91	148,95	10,03	263,6	III	199,3	III
17	P	39,46	50,53	29,88	100,78	20,38	398,5	II	319,4	III
18	Q	15,54	50,50	30,43	101,64	20,60	351,9	II	287,5	II
19	R	28,23	65,96	30,11	100,34	20,45	357,0	II	307,6	III
20	S	28,44	35,49	30,18	100,54	20,48	391,4	II	323,2	III
21	T	28,06	50,34	44,36	100,92	20,38	252,9	IV	270,8	III
22	U	28,50	50,04	16,27	100,59	20,43	413,3	II	361,0	II
23	V	28,44	50,80	29,79	150,44	20,51	415,3	II	344,5	II
24	W	29,06	50,66	29,68	50,27	20,46	231,2	III	211,2	IV
25	X	29,45	50,00	29,53	101,43	30,13	420,9	II	387,0	II
26	Y	28,80	49,91	29,81	99,42	10,36	228,6	IV	106,6	IV
27	Z	28,04	50,61	30,08	100,87	20,39	425,1	II	359,7	III
28	Ż	28,30	50,64	29,64	101,49	20,92	285,3	II	222,2	II
29	Ź	28,23	50,46	29,69	101,30	20,63	379,5	II	317,0	II

Comparison of the test results with an analytical model

For investigated specimens, calculations of the resistance according to the analytical model introduced in p. 2. were performed. Calculations were carried out for the nominal resistance on the bolts, real geometric dimensions and steel strength of the specimens. Results of calculations were given in table 3. In the table one gave also mode of failure for T-stub as a related to the minimum values of their strength. Results of the resistance of specimen received from experimental research and from the analytical model do not differ than few percent. The exceptions are only for I and IV mode of failure. In I mode of failure the resistance of T-stub is govern by the bolts, for which a nominally values of the strength was adopted. The difference here amounts to 31%. Resistance of the specimen with IV mode of failure is understated in the analytical model. In this case the resistance of the T-stub is estimated based on the yield strength of steel. The resistance is related to first plastifying of the T-stub and not to the maximum tensile force.

Conclusion

Experimental tests showed that in real joints could appear all four modes of failure which became established in the analytical model. They define also that the strength of T-stub is related to maximum tensile force or first plastifying of the flange.

Real deformations of the T-stub will be used to estimate real rotation capacity of the whole joint.

Presented analytical model for assessment of the resistance of the joint with four bolts in each row can be used in the component method preferred in actual design standards.

1. PN-EN 1993-1-8 Eurocode 3 (2005) Design of Steel Structures. Part 1-8 Design of Joints. CEN. 2. Kozłowski A. Pisarek Z (2008) Resistance and stiffness of T-stub with four bolts. Archives of Civil Engineering Liv. 1: 167-191. 3. Krumm R (1991) Calculation of rigid face plate connections according to the DSTV/DASt Guidelines. Stahlbau 60: 4. Ungermann D, Schmidt B (2005) Moment resistance of bolted beam to column connections with four bolts in each row. Procc. of IV European Conference on Steel and Composite Structures, Eurosteel, Maastricht: 5. Polanski Z (1984) Planowanie doświadczalne w technice. PWN, Warsaw. (in Polish).

UDC 662.997

B.I. Piznak, V.M. Zhelykh, V.Z. Pashkevych
Lviv Polytechnic National University
Department of Heat and Gas Supply, and Ventilation

THE ECONOMIC EFFICIENCY OF THE USE OF POLYMERIC MATERIALS IN THE DESIGN OF SOLAR COLLECTORS

The results of the technical and economic analysis of the use of flat solar collector based on polymeric materials are given.

Key words: energy-savings, solar collector, polymeric materials, cellular polycarbonate plate.

Наведено результати техніко-економічного аналізу використання плоского сонячного колектора на основі полімерних матеріалів.

Ключові слова: енергозбереження, сонячний колектор, полімерні матеріали, стільникова полікарбонатна плита.

Timeliness

For the last centuries the demands for the energy quantity have increased in an unprecedented manner and the mankind is looking for additional energy sources. The increase in energy consumption occurs due to the constant population growth and the need for development and greater comfort.

Energy problem could be solved either by the sustainable use of the available natural energy sources, i. e. by conducting energy and resource saving policy or by using new alternative and renewable energy sources.

Most developed countries are involved in the implementation of alternative energy sources of sun, wind, flow, heat of the earth core etc. They cannot fully substitute oil, gas, coal or nuclear energy and have to be used along with the traditional energy sources. Moreover, they can have a crucial role in the regions with favorable climate conditions. The main reason restraining the development of renewable energy sources is the necessity of high capital expenditure.

Currently the most effective way for the development of the alternative energy is the usage of solar energy to obtain the heat. Transition to the solar energy prevents from the emission of carbon dioxide, carbon monoxide, sulfur dioxide, nitrous oxide and other pollutants into the atmosphere. The climate of Ukraine provides the possibility for the wide use of solar energy. The annual radiative solar flux at 1 m^2 of horizontal surface in the southern regions of Ukraine constitutes 1100-1380 kWh, and the duration of solar radiation comprises approximately 2000 hours per year [1]. Therefore, the conception of accelerated development of domestic solar installations to obtain heat energy is entirely appropriate. A number of solar heat supply engineering systems have been already developed and they are being developed now, however, they all have one mutual element which is a solar collector. The effectiveness of solar installation depends mainly on the right choice of the collector.